Penetration of convective plumes into a strongly stably stratified region

Charles Powell, Peter Haynes, John Taylor

DAMTP, University of Cambridge

Background

We consider the problem of a buoyant plume, generated in an unstratified region, impinging on a region with strong stable stratification. This is a simple representation of the tropical upper troposphere and lower stratosphere (UTLS), where convective plumes generated by strong thunderstorm complexes can penetrate into the lower stratosphere. Stratospheric composition is largely set by cross-tropopause transport in the tropics as tropospheric air predominantly enters the stratosphere in the tropics (Fueglistaler et al., 2009). Detailed numerical simulation of entire thunderstorm complexes is computationally expensive (Dauhut et al., 2015, 2018); the working hypothesis here is that it is useful to study the idealised fluid dynamics problem of penetration of a single artificially generated plume into a stably stratified layer.

Verification of numerical simulation: plume dynamics in an unstratified environment

Large eddy simulations are performed using DIABLO, a Fortran incompressible Navier-Stokes solver, in a doubly periodic domain. A plume with a fixed buoyancy flux and source radius is generated by relaxing the buoyancy towards the analytic buoyancy profile of a pure plume in a thin forcing region. Turbulence is initiated with a random 5% perturbation of all velocity components in a thin layer above the forcing region. The capability to represent plume dynamics is verified by comparison with DNS of a plume in an unstratified environment in the literature (van Reeuwijk et al., 2016). We use self-similarity, stationarity and azimuthal symmetry to examine integral quantities representing the volume, momentum and buoyancy flux ($\boldsymbol{Q}, \boldsymbol{M}, \boldsymbol{F}$) (Morton et al., 1956), as well as dynamical variables of vertical velocity, buoyancy, radial momentum and buoyancy fluxes ($\overline{w}, \overline{b}, \overline{u'w'}, \overline{u'b'}$). The figure shows non-dimensionalised, azimuthally averaged profiles of these variables at a range of vertical heights. Here, $\overline{\cdot}$ represents an azimuthal and time average.

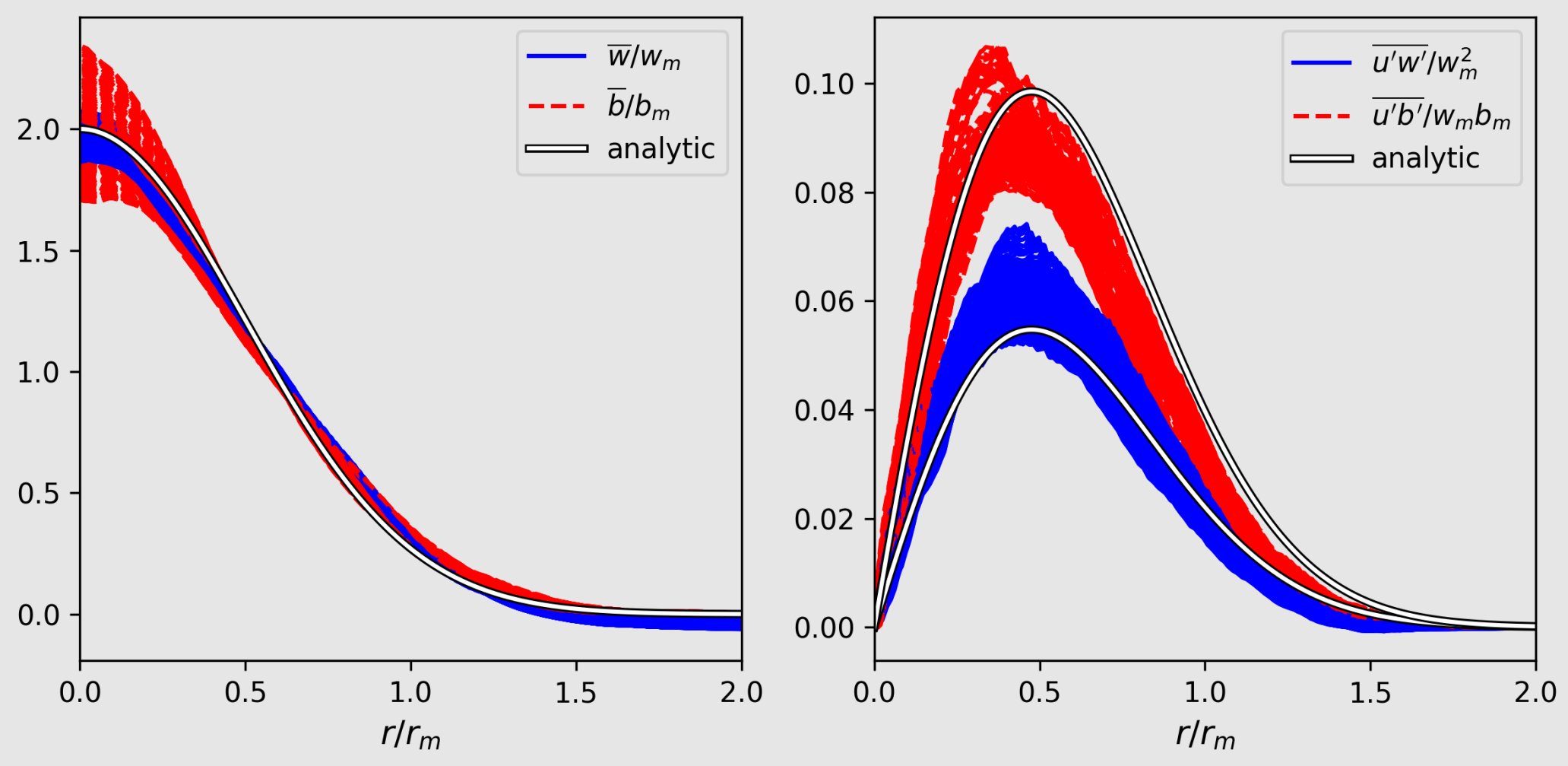

Figure: Vertical velocity and buoyancy (left), radial momentum and buoyancy flux (right)

Penetration into a stably stratified environment

We introduce a linear stably stratified layer with buoyancy frequency $N^2 = \partial_z b$ at a height H above the lower boundary as a simple representation of the UTLS. The choice of N^2 and the source buoyancy flux F_0 is used to non-dimensionalise the problem in the stratified region. This simple setup is studied experimentally by Ansong and Sutherland (2010), parameters from which are used as a baseline for the LES domain size and forcing. Their experimental results are compared with LES results as verification; calculations of the maximum penetration height z_{max} and equilibrium height z_{eq} (at which the intrusion forms) agree qualitatively.

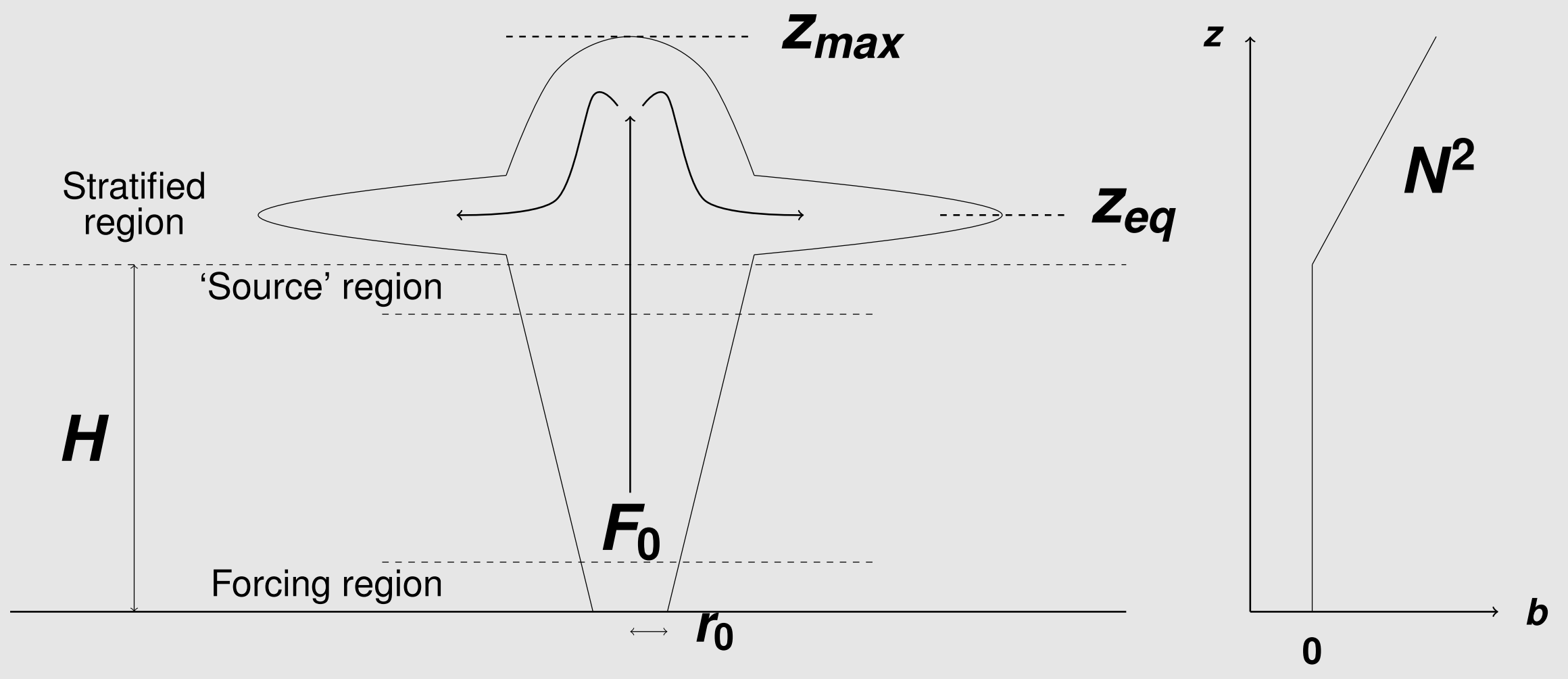

Tracer vs. buoyancy distribution

We examine mixing processes by considering the distribution of a passive tracer in buoyancy coordinates. Comparing the distribution in the stratified region post-penetration at multiple times (shaded lines, times non- dimensional) with the distribution in a 'source' region pre-penetration (black dashed line) indicates the redistribution of tracer due to mixing. Curves are normalised to account for the increase in total tracer with time; the distribution shape is the key property. As plume fluid enters the stratified region, it eventually settles at an equilibrium height z_{eq} where an intrusion forms, resulting in a peak at low buoyancies in the distribution. The distribution tail grows as plume fluid mixes with more buoyant fluid at the maximum penetration height z_{max}. The tracer probability at low buoyancies decreases post-penetration due to the strong stratification; most low-buoyancy fluid parcels will quickly encounter fluid of greater buoyancy. Future work will consider scalings for the buoyancy range where tracer is redistributed.

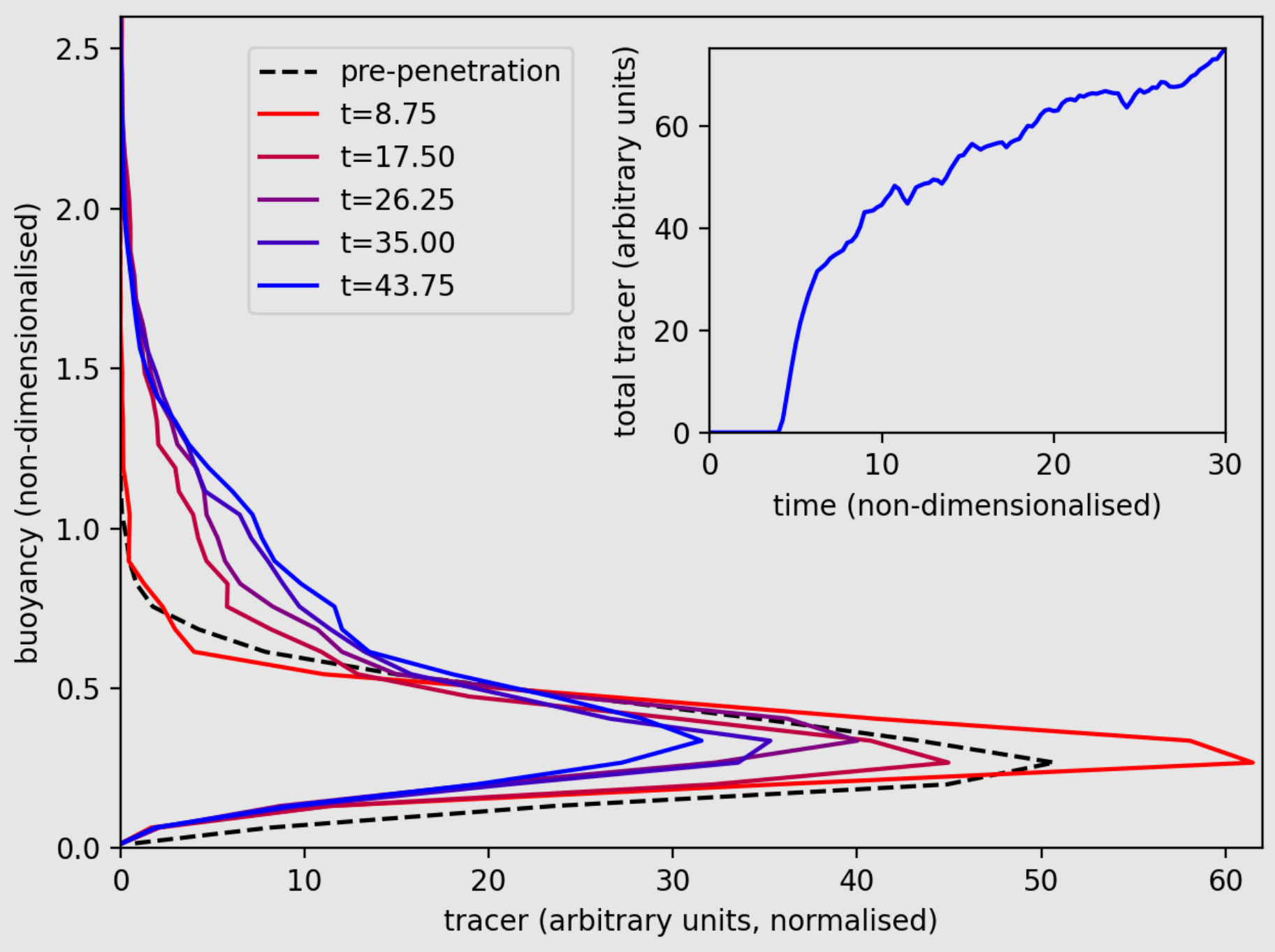

Figure: tracer probability distribution in buoyancy coordinates in stratified region

Estimates of maximum penetration height

The maximum penetration height into the stratified region is of central importance in this problem, as it determines the level of fluid detrainment (Ansong et al., 2008) and in the atmospheric case, it is directly linked to temperature constraints on concentration (Jensen et al., 2007). To estimate this height, Ansong and Sutherland (2010) numerically solve the plume equations for the fluxes. Whilst the estimates correlate with experimental values, the flux profiles themselves are qualitatively different. A simple dimensional analysis fit to LES gives $z_{max} \propto \alpha^{-1/2} F_0^{1/4} N^{-3/4}$ (Devenish et al., 2010). An energetic argument, assuming all KE at penetration is converted to PE, gives $z_{\mathrm{max}} \propto N^{-1} H^{-1/3} F_0^{1/3}$. The predictions for z_{max} from these three methods are shown here on a cross-section of a penetrating plume with tracer contours overlaid and the forcing region indicated. Results from the plume equations demonstrate systematic underprediction of z_{max} whilst dimensional analysis predictions tend to overpredict.

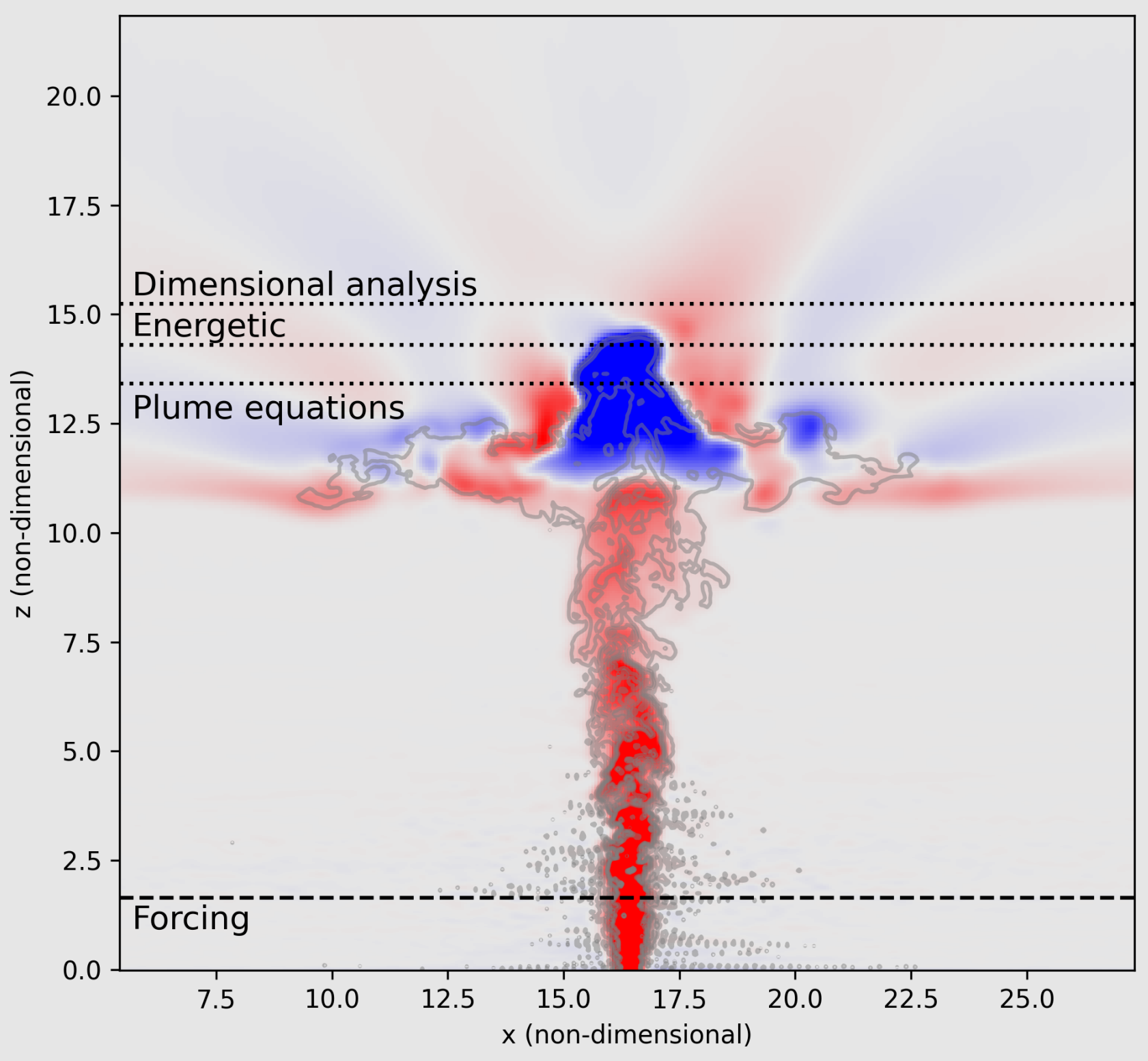

Figure: Penetrating plume buoyancy cross-section with tracer contours (grey). Background buoyancy profile subtracted.

Gravity wave generation and mixing

In cross-sections of the buoyancy field with the environmental profile subtracted (above), internal gravity waves are apparent in the stratified region. A sponge layer prevents interference from reflections. Future work will quantify their contribution to mixing, in particular the spatial characteristics, and the effect of their modification of the environment on tracer transport. (Lane and Reeder, 2001)

References

J. K. Ansong and B. R. Sutherland. Internal gravity waves generated by convective plumes. *J. Fluid Mech.*, 648:405–434, 2010.

J. K. Ansong, P. J. Kyba, and B. R. Sutherland. Fountains impinging on a density interface. *J. Fluid Mech.*, 595:115–139, 2008.

T. Dauhut, J.-P. Chaboureau, J. Escobar, and P. Mascart. Large-eddy simulations of Hector the convector making the stratosphere wetter. *Atmos. Sci. Lett.*, 16(2):135–140, 2015.

T. Dauhut, J-P. Chaboureau, P. H. Haynes, and T. P. Lane. The mechanisms leading to a stratospheric hydration by overshooting convection. *J. Atmos. Sci.*, 75(12):4383 – 4398, 2018.

B. J. Devenish, G. G. Rooney, and D. J. Thomson. Large-eddy simulation of a buoyant plume in uniform and stably stratified environments. *J. Fluid Mech.*, 652:75–103, 2010.

S. Fueglistaler, A. E. Dessler, T. J. Dunkerton, I. Folkins, Q. Fu, and P. W. Mote. Tropical tropopause layer. *Rev. Geophys.*, 47(1), 2009.

E. J. Jensen, A. S. Ackerman, and J. A. Smith. Can overshooting convection dehydrate the tropical tropopause layer? *J. Geophys. Res. Atmos.*, 112(D11), 2007.

T. P. Lane and M. J. Reeder. Convectively generated gravity waves and their effect on the cloud environment. *J. Atmos. Sci.*, 58(16):2427–2440, 2001.

B. R. Morton, G. I. Taylor, and J. S. Turner. Turbulent gravitational convection from maintained and instantaneous sources. *Proc. R. Soc. Lond. Ser. A*, 234 (1196):1–23, 1956.

M. van Reeuwijk, P. Salizzoni, G. R. Hunt, and J. Craske. Turbulent transport and entrainment in jets and plumes: A DNS study. *Phys. Rev. Fluids*, 1: 074301, 2016.

`Atmosphere & Ocean Dynamics group`

`cwp29@cam.ac.uk`